SAND2022-1355C

Sandia National Laboratories

Magneto-Acoustic Waves in Multiferroic Heterostructures

Sidhant Tiwari (Postdoctoral Appointee, stiwar@sandia.gov)

PI: Darren W. Branch (Distinguished Member of Technical Staff)

Biological and Chemical Sensors Department, 08634

Sandia National Laboratories, Albuquerque, NM 87122

TANMS Advanced Research Strategy Meetings

February 8th, 2022

U.S. DEPARTMENT OF ENERGY NNSA

Motivation: RF Micro-Magnetic Devices

RF Magnetic Devices

X-Band Radar T/R Module

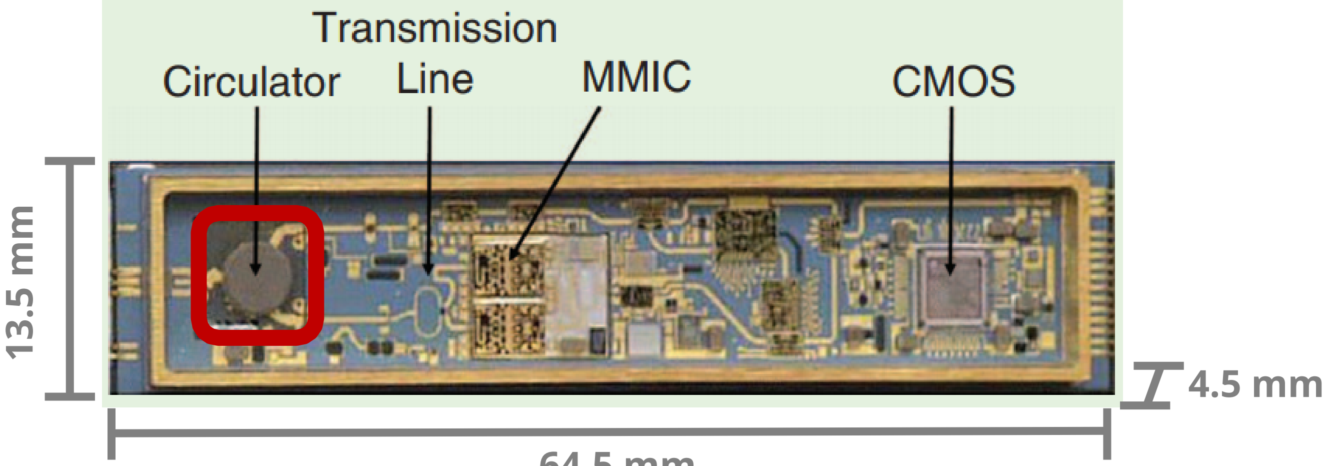

Palmer, W., et al., IEEE MM (2019)

1.7 GHz Antenna

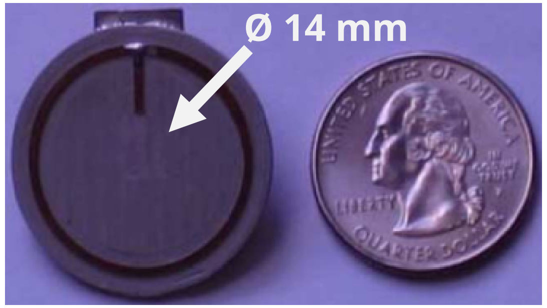

Yang, G.M., IEEE AP (2009)

400 – 800 MHz FSL

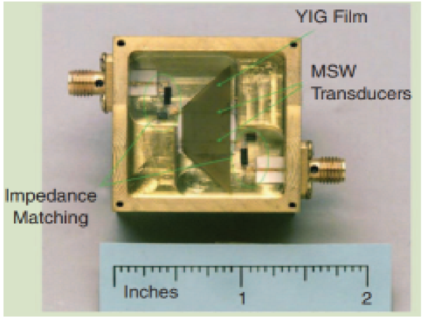

Adam, J.D., IEEE MM (2014)

3.4 GHz SNE

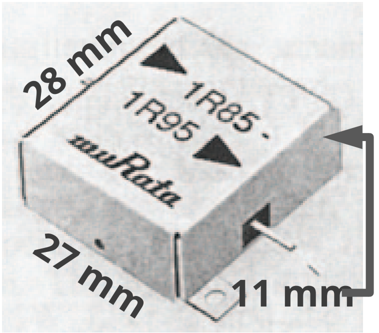

Adam, J.D., IEEE MM (2014)

RF Acoustic Devices

$$\lambda_{acoustic} \approx 10^{-5} \lambda_{EM}$$

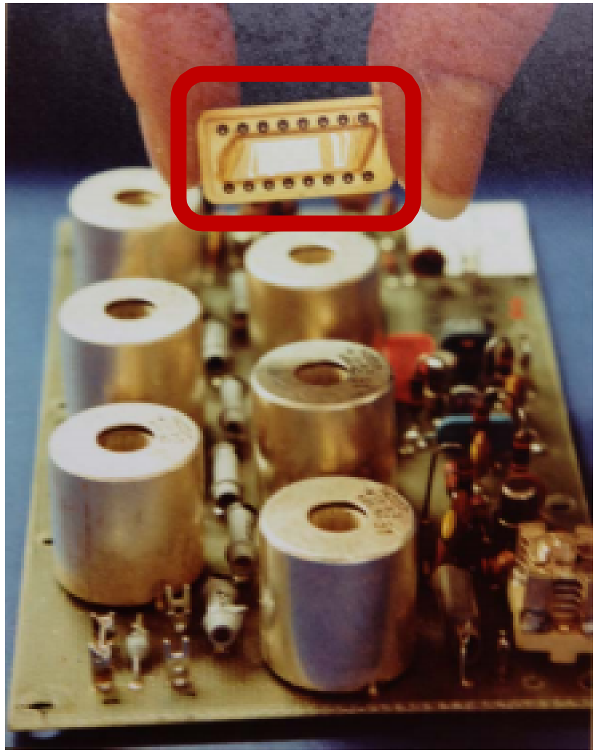

Ruppel, C.C.W., IEEE UFFC (2017)

Magneto-acoustics will enable micro-scale RF magnetic devices!

Outline

Lamb Waves for High Frequency Multiferroics

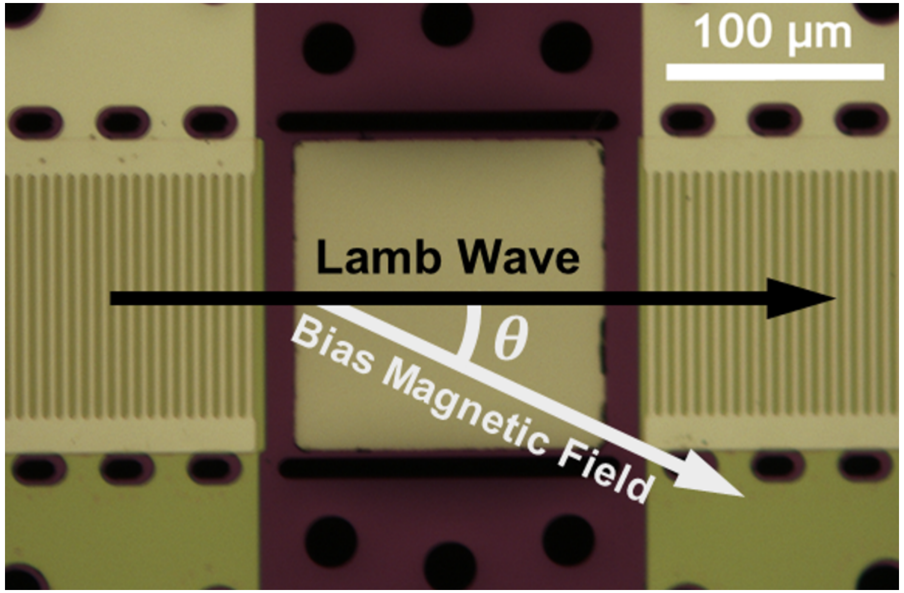

Tiwari, S., et al., JMEMS (2020)

Rapid Modelling of Magneto-Acoustic Devices

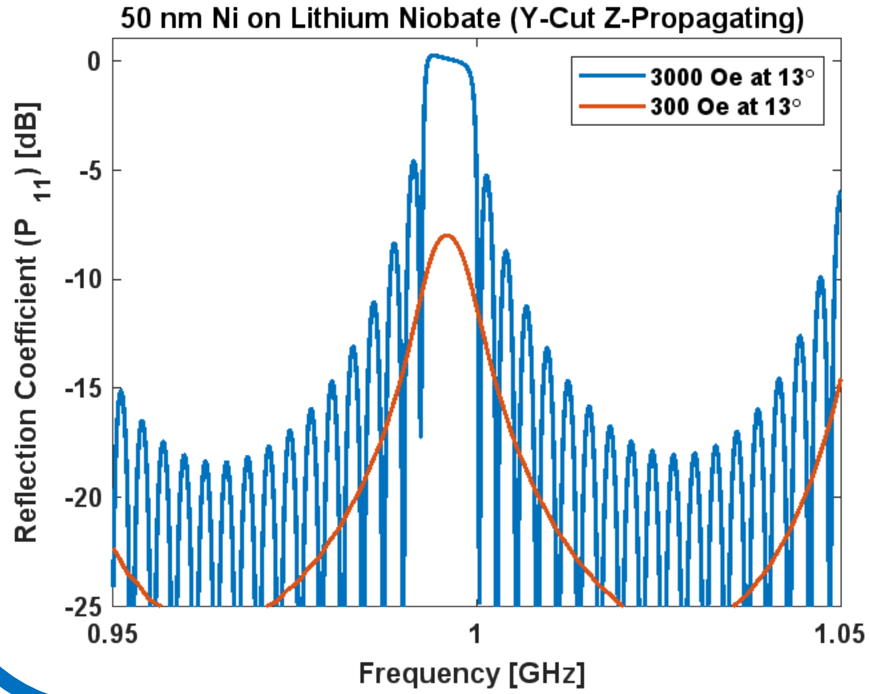

Outline

Lamb Waves for High Frequency Multiferroics

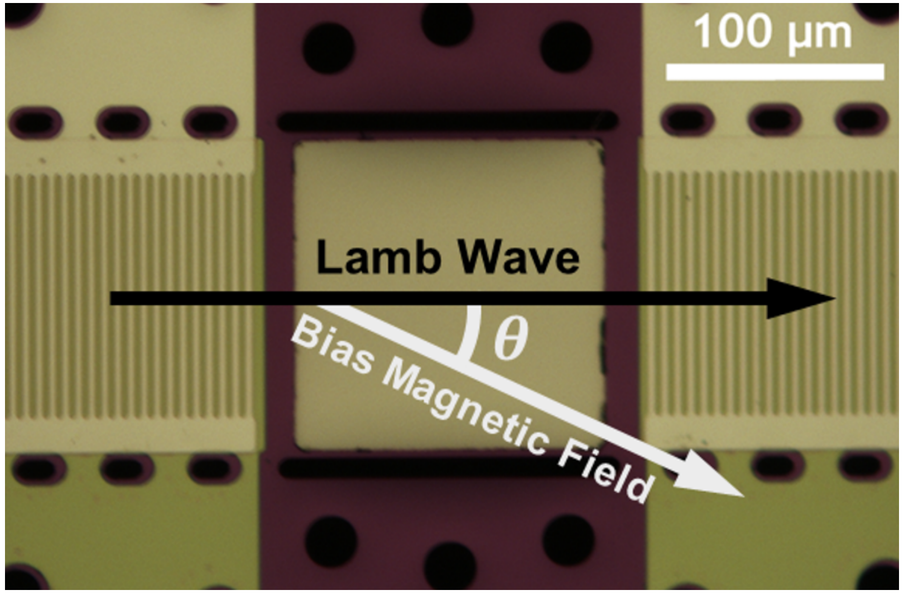

Tiwari, S., et al., JMEMS (2020)

Rapid Modelling of Magneto-Acoustic Devices

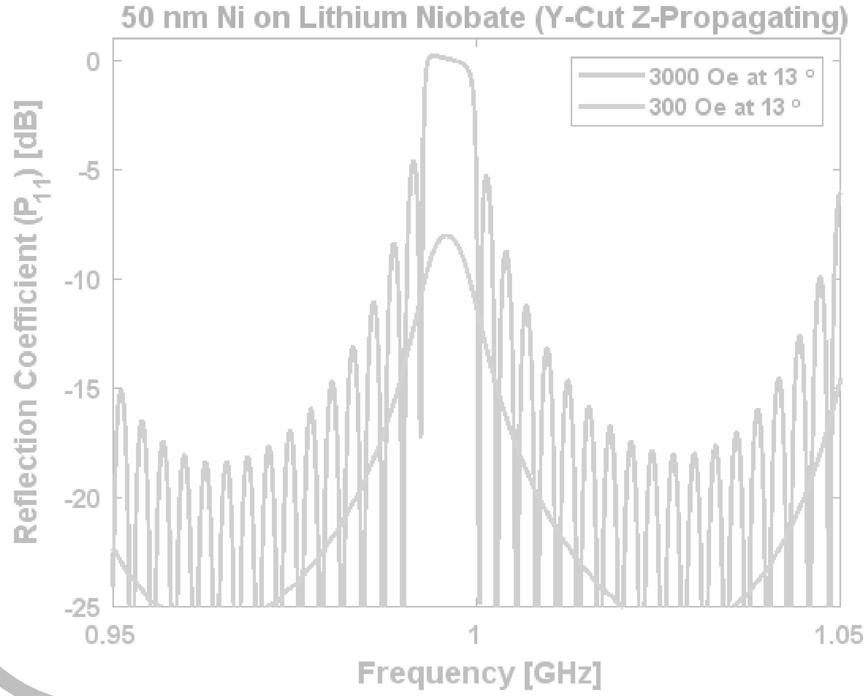

Background: Multiferroic Surface Acoustic Wave Devices

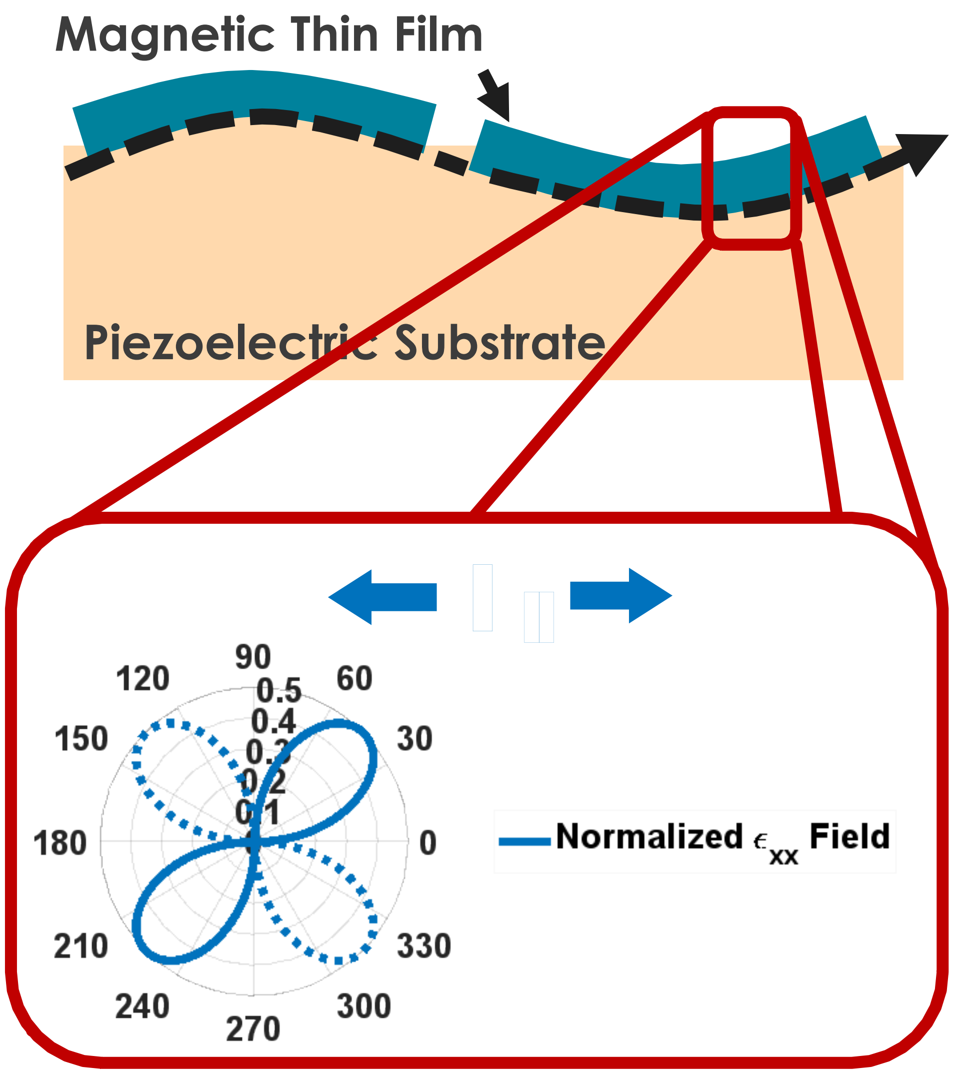

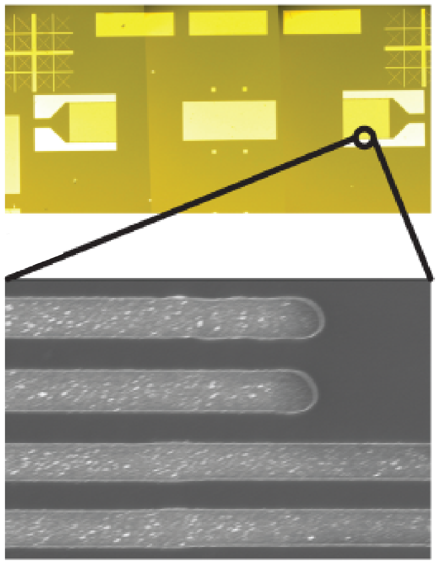

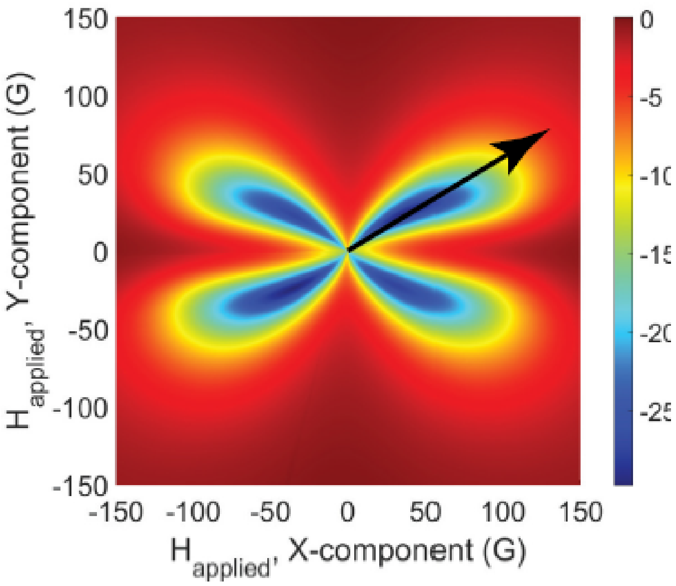

Labanowski, D., et al., APL (2016)

Pros:

- Simple and cheap to fabricate
- Mechanically robust

Cons:

- Low coupling coefficient (compared to bulk modes)
- Difficult to scale to higher frequencies (>1 GHz)

Lamb Waves for High Frequency Multiferroic Devices

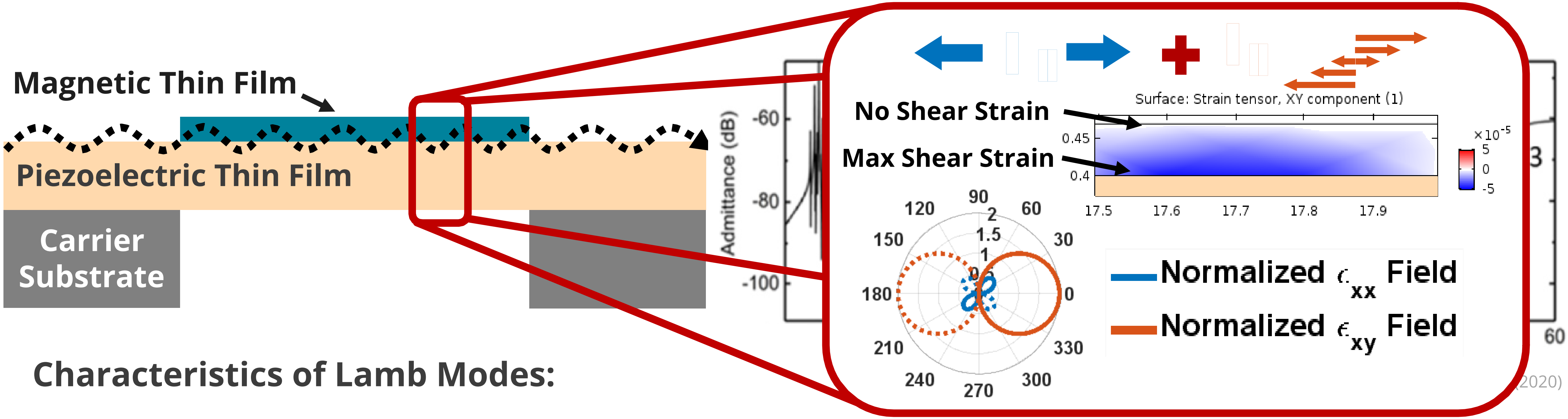

Characteristics of Lamb Modes:

- Higher piezoelectric coupling coefficients than SAW based devices
  (Makes higher harmonics viable for device applications)
- Higher wave velocities means easier lithography and higher frequencies
  (Devices have been demonstrated up to 55 GHz!)
- Multiple types of Lamb modes give greater design flexibility
  (Different strain profiles will give rise to different coupling profiles)
- Thin waveguide cross-sections give rise to steep strain gradients in thin-film overlays

Acoustic Wave Coupling to Spin Wave Modes

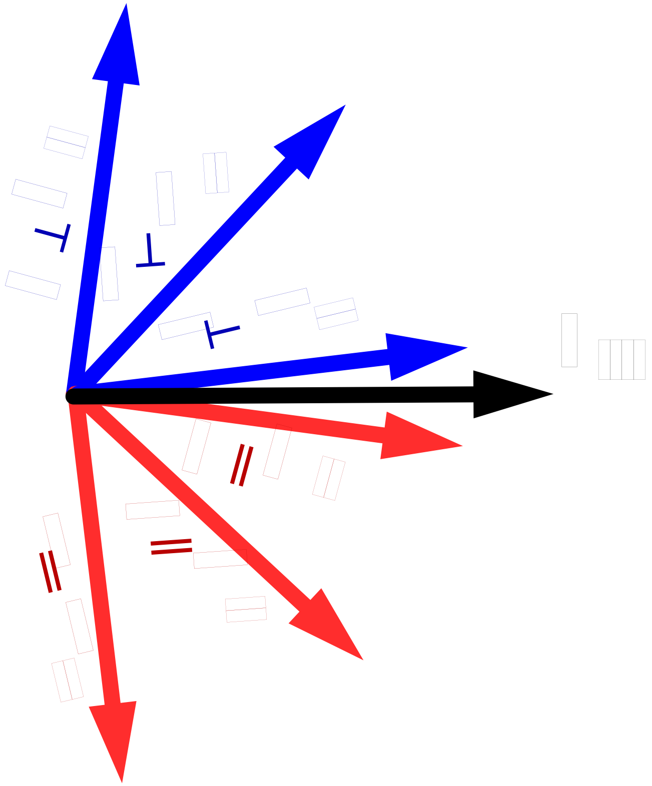

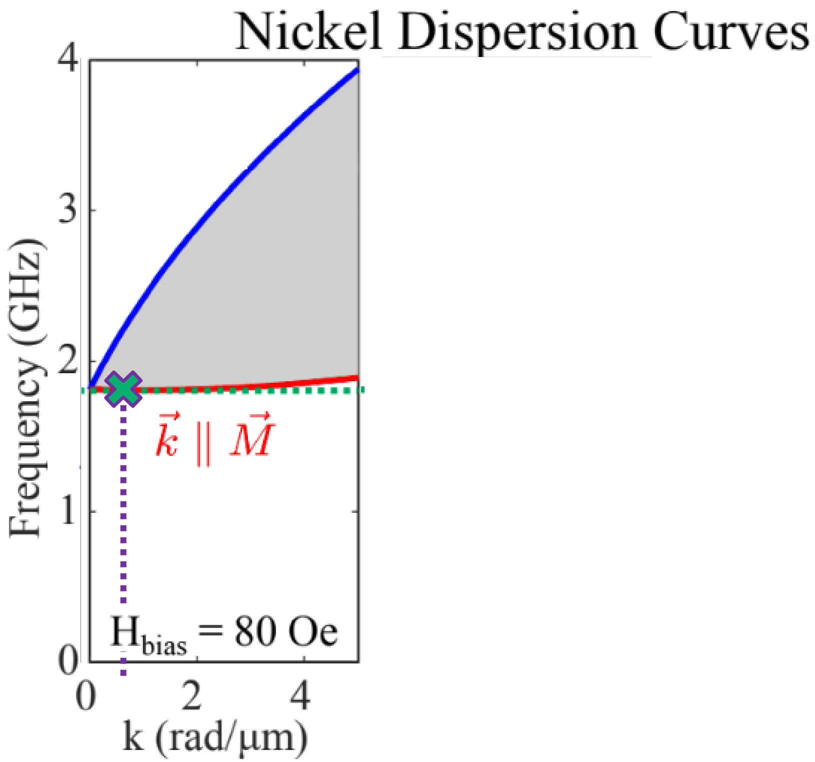

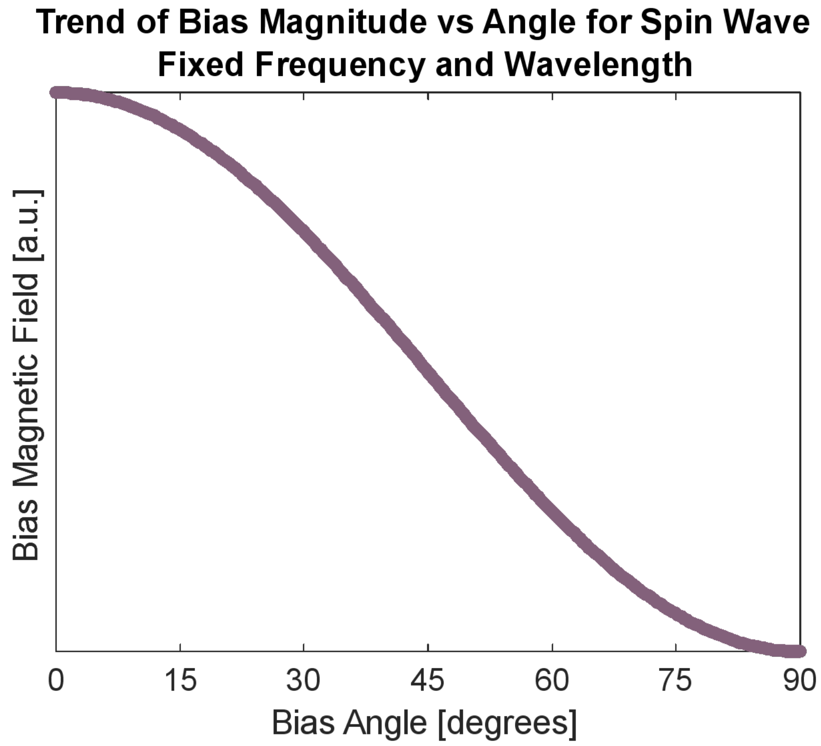

Adapted from Nygren, K., et al., APS (2019)

- Highly nonuniform strain profiles are better described as coupling to spin waves instead of ferromagnetic resonance
- $\vec{k}$ vector of the spin wave is set by the Lamb wave, with the magnetic field bias magnitude (H_{bias}) being determined by the relative angle of the bias field

Characterization of Lamb Wave Delay Line

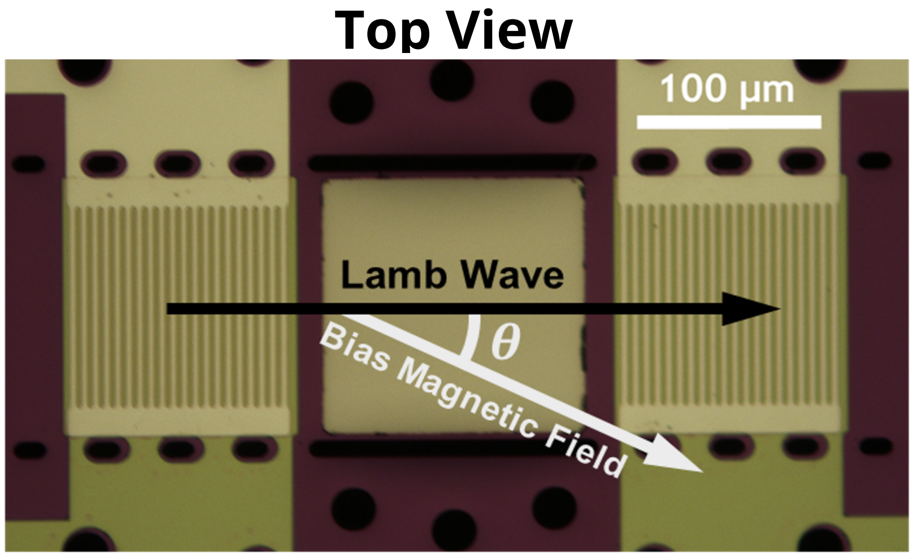

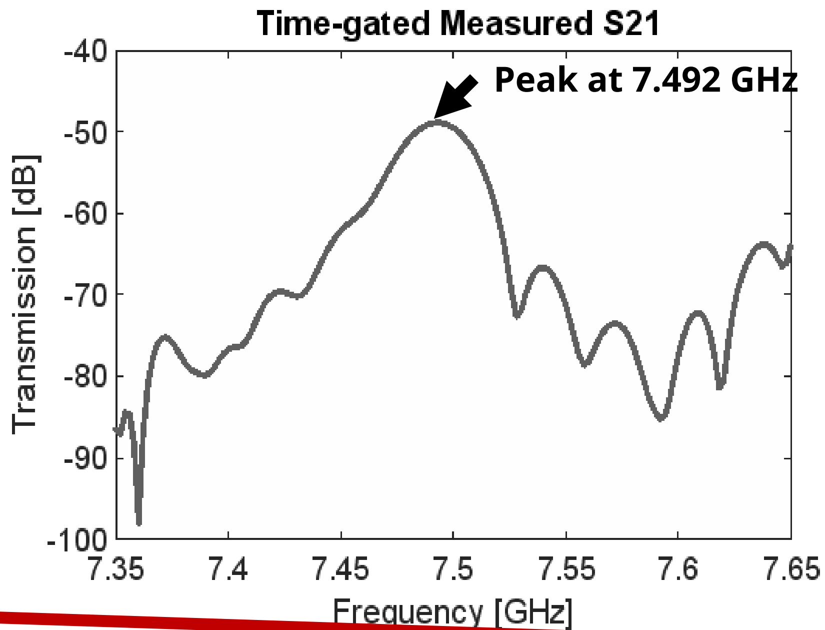

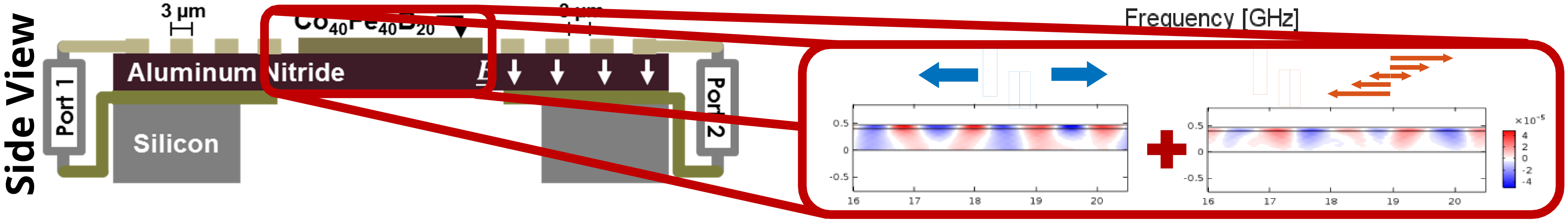

- Delay structure is a stack of Aluminum Nitride (400 nm) and CoFeB (70 nm), 144 μm square
- Chosen mode of propagation is a symmetric Lamb mode at ~7.5 GHz
- Change in insertion loss measured as a function of bias magnitude and angle
- IFBW is set to 500 Hz and averaging is set to 10 points to maximize sensitivity

Characterization Results

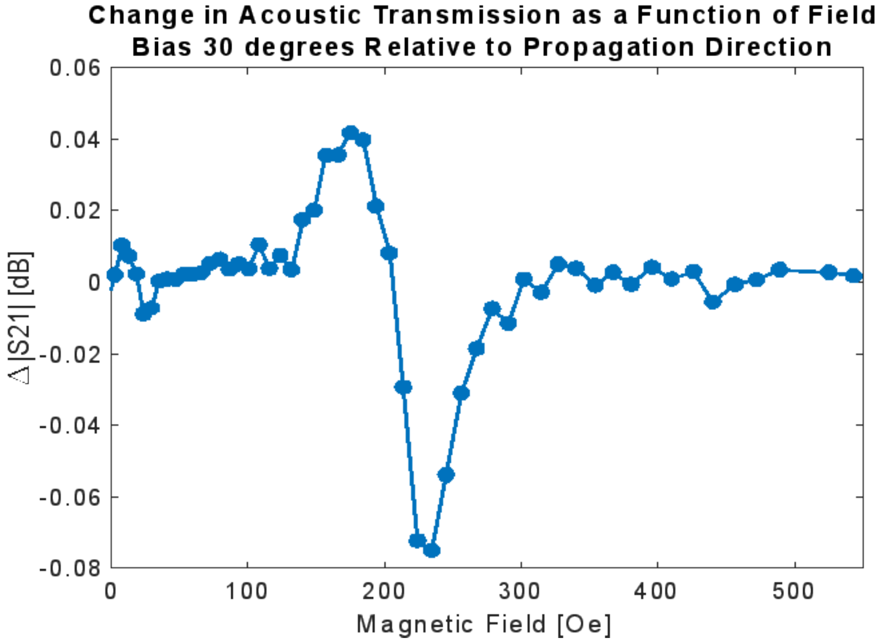

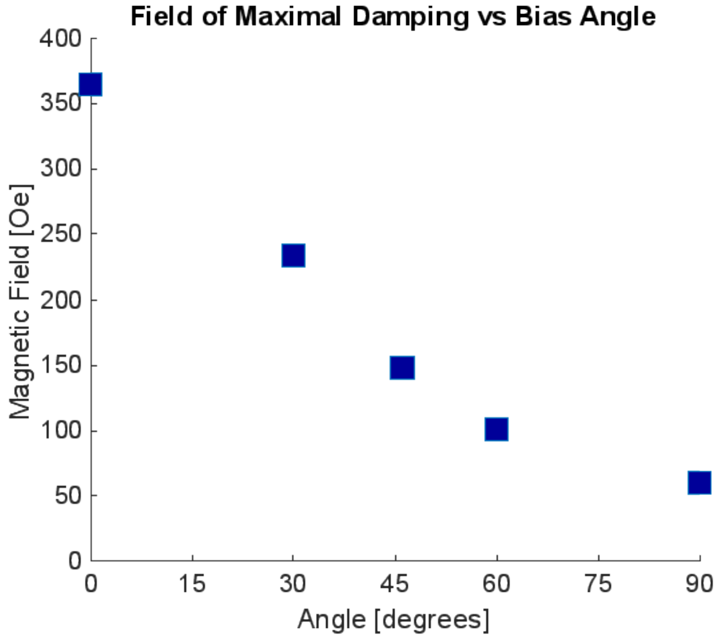

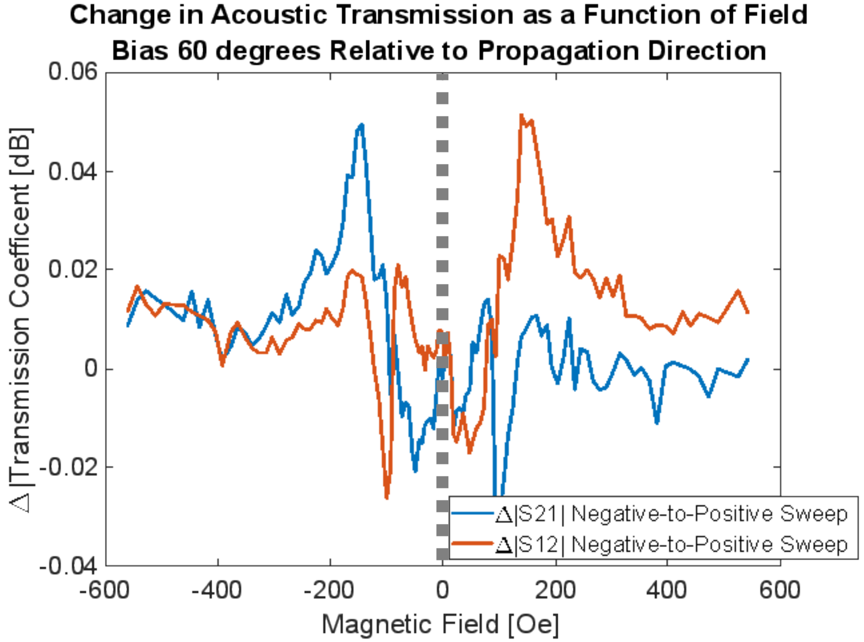

- As in typical ADFMR experiments, loss increases at a particular bias
- Transmission is found to increase at a particular bias, attributed to wave velocity increase
- As bias angle is increased, the bias magnitude for maximum absorption decreases, consistent with spin wave theory
- Nonreciprocal transmission has also been demonstrated, but the physics behind it has yet to be determined

Outline

Lamb Waves for High Frequency Multiferroics

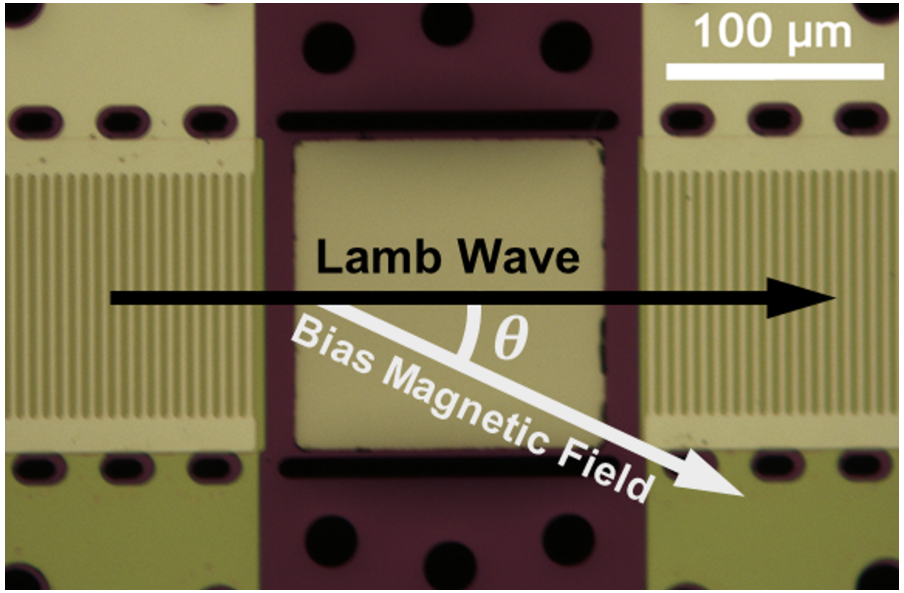

Tiwari, S., et al. (JMEMS, 2020)

Rapid Modelling of Magneto-Acoustic Devices

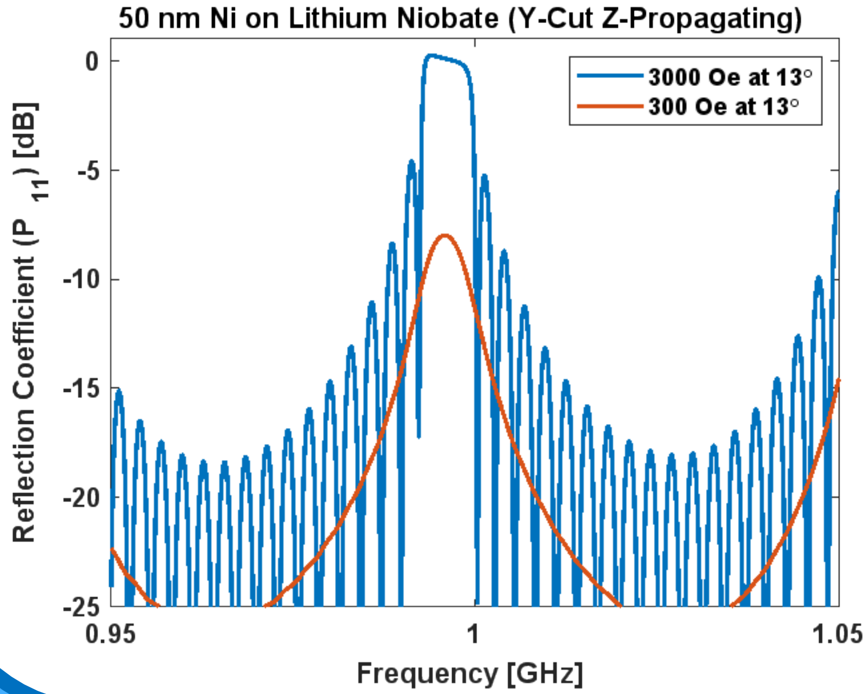

Background: Modelling for RF Multiferroic Devices

Finite-Difference Time-Domain

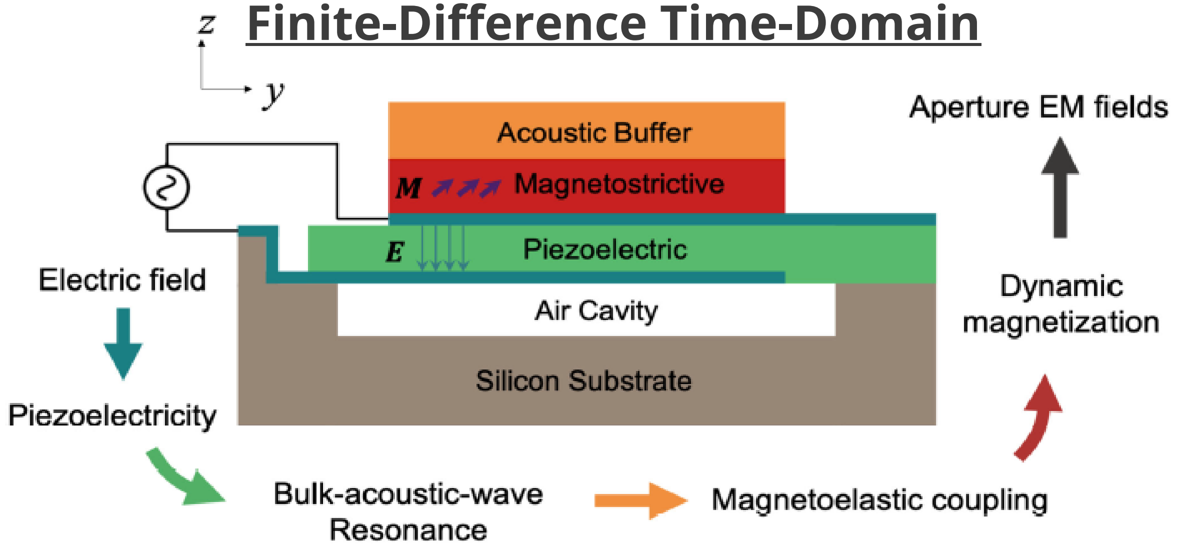

Yao, Z., et al., IEEE JMMCT (2020)

Finite Element Analysis

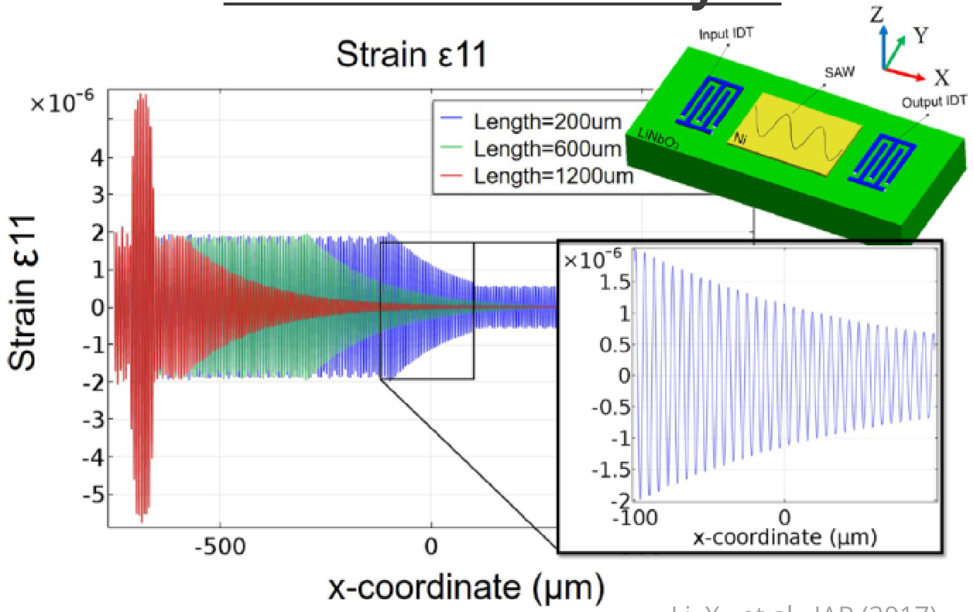

Li, X., et al., JAP (2017)

Pros:

- Robust in regards to acoustic wave mode chosen
- Can simulate transients (FDTD) and nonlinearity (FDTD)
- Flexible simulation geometry (FEA)

Cons:

- Very slow and resource intensive for practical device scale

Propagation Constant Perturbation

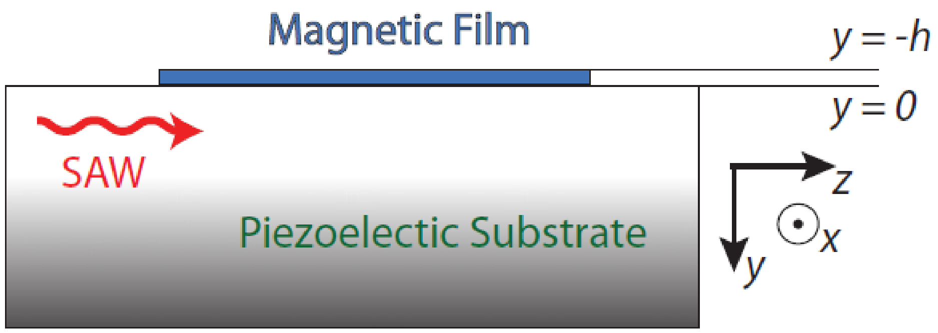

Gowtham, P.G., et al., PRB (2016)

P-Matrix Modelling of Acoustic Devices

Acoustic wave devices are built out of many arrayed elements, making the structures many of wavelengths long

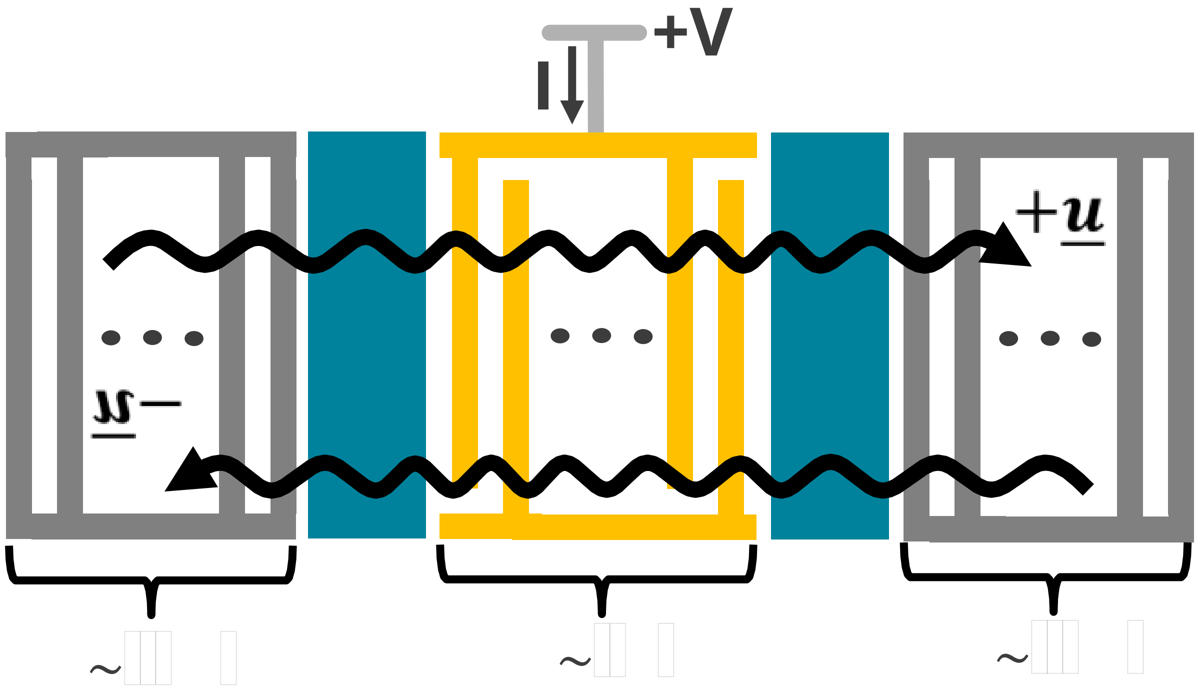

P-matrices model the combined electrical and acoustic response of a single element

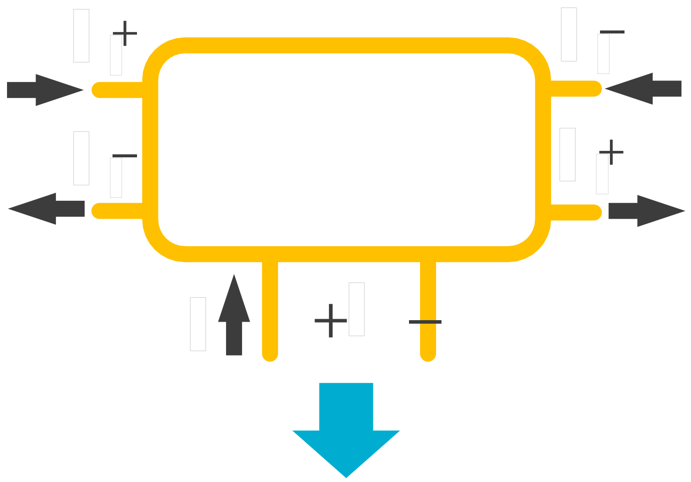

$$\begin{bmatrix} u_1^- \\ u_2^+ \\ I \end{bmatrix} = \begin{bmatrix} P_{11} & P_{12} & P_{13} \\ P_{21} & P_{22} & P_{23} \\ P_{31} & P_{32} & P_{33} \end{bmatrix} \begin{bmatrix} u_1^+ \\ u_2^- \\ W \end{bmatrix}$$

- P-matrices can be derived for elements via FEA, coupling of modes, perturbation theory, etc
- ***Once P-matrix elements are built, they can be cascaded to rapidly simulate complex acoustic devices***
- ***With a P-matrix for a magneto-acoustic element derived, the technique can be used to rapidly design magneto-acoustic devices***

Wave Scattering due to Magnetic Thin-Film

Magneto-Elastic Equations of Motion

$$\dot{\underline{m}} = -\mu_0\gamma\left\{\underline{m}\times\underline{H}_{bias} + \underline{M}_{DC}\times\left(\underline{h} - \underline{\underline{N}}\,\underline{m} + \mu_0^{-1}\underline{\underline{\underline{p}}}\,\underline{\underline{S}}\right)\right\}$$

$$\rho\ddot{\underline{u}} = \underline{\nabla}\cdot\underline{\underline{T}}$$

$$\underline{\underline{T}} = \underline{\underline{\underline{\underline{c}}}}_M\underline{\underline{S}} + \underline{\underline{\underline{q}}}\,\underline{m}$$

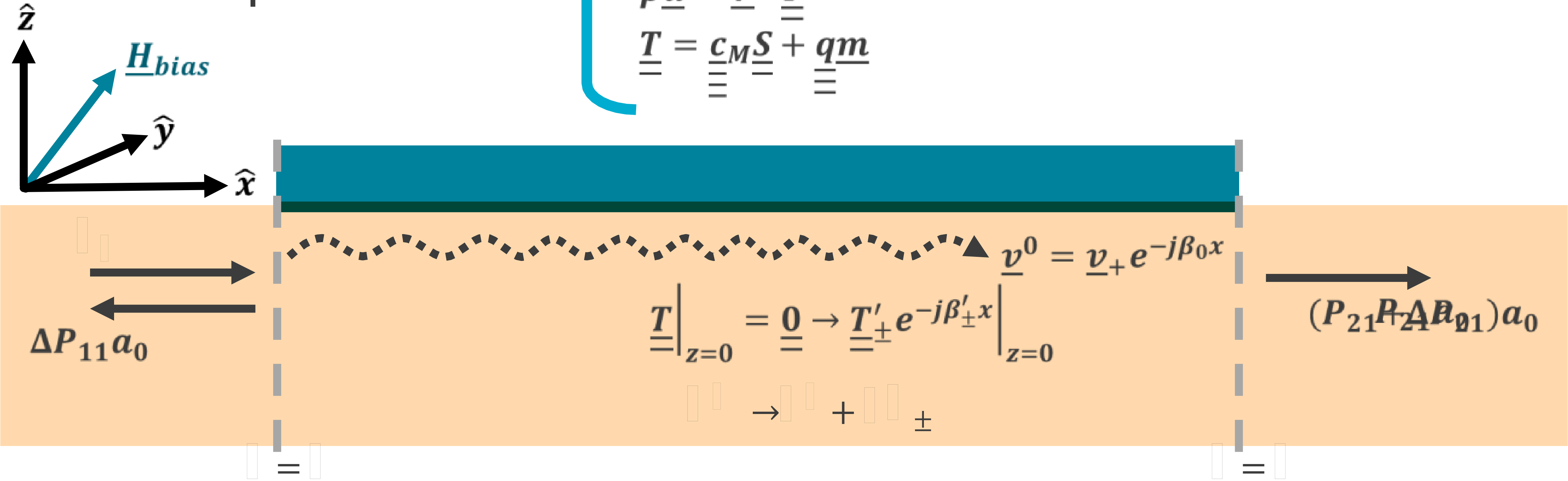

Once surface stress is found, calculation of scattering coefficients is straight forward

$$\Delta\beta_\pm = \left(\underline{v}_\pm\cdot\left.\underline{\underline{T}}'_\pm\right|_{z=0}\right)\cdot\hat{z} \qquad \Delta P_{ij} = \frac{1}{4}\int_0^l\left(\underline{v}_i^0(x)\cdot\left.\underline{\underline{T}}'_j(x)\right|_{z=0}\right)\cdot\hat{z}\,dx$$

Calculation of Surface Perturbation from Magnetic Film

Magneto-Acoustic Stiffness

$$\underline{\underline{c}}_{\pm}(\omega, \underline{H}_{bias}) = \underline{\underline{c}}_{M} + \underline{\underline{\Delta c}}_{\pm}(\omega, \underline{H}_{bias}) = \underline{\underline{c}}_{M} - \mu_0^{-1} \underline{\underline{p}}_{\pm}^{T}(\underline{H}_{bias}) \underline{\chi}_{e,\pm}(\omega, \underline{H}_{bias}) \underline{\underline{p}}_{\pm}(\underline{H}_{bias})$$

- χ_e is the "external susceptibility", which already includes RF demagnetization fields
- χ_e is not symmetric, meaning the stiffness tensor is no longer symmetric, so $\boldsymbol{T_{ij} \neq T_{ji}}$ ***cannot be assumed***
- Dependence on ϕ means waves travelling in the $+x$ ***and*** $-x$ ***don't necessarily see the same stiffness***

Solution for Surface Stresses

System of Equations:

$$\frac{\partial T'_{xi}}{\partial x} + \frac{\partial T'_{zi}}{\partial z} = -\rho\omega^2 u_i$$

$$T'_{ij} = c_{ijkl,\pm} \cdot \frac{1}{2}\left(\frac{\partial u_i}{\partial x_j} + \frac{\partial u_j}{\partial x_i}\right)$$

Boundary Conditions:

$$T'_{zi}\Big|_{z=h} = 0$$

$$j\omega \cdot u_i\Big|_{z=0} = v_{i\pm}$$

Tabulated for most common modes. Can be easily calculated for others.

$$\frac{\partial}{\partial z}\begin{bmatrix} u_x \\ u_y \\ u_z \\ \frac{j}{\beta}\frac{\partial u_x}{\partial z} \\ \frac{j}{\beta}\frac{\partial u_y}{\partial z} \\ \frac{j}{\beta}\frac{\partial u_z}{\partial z} \end{bmatrix} = \underline{\underline{A}}_{\pm} \begin{bmatrix} u_x \\ u_y \\ u_z \\ \frac{j}{\beta}\frac{\partial u_x}{\partial z} \\ \frac{j}{\beta}\frac{\partial u_y}{\partial z} \\ \frac{j}{\beta}\frac{\partial u_z}{\partial z} \end{bmatrix}$$

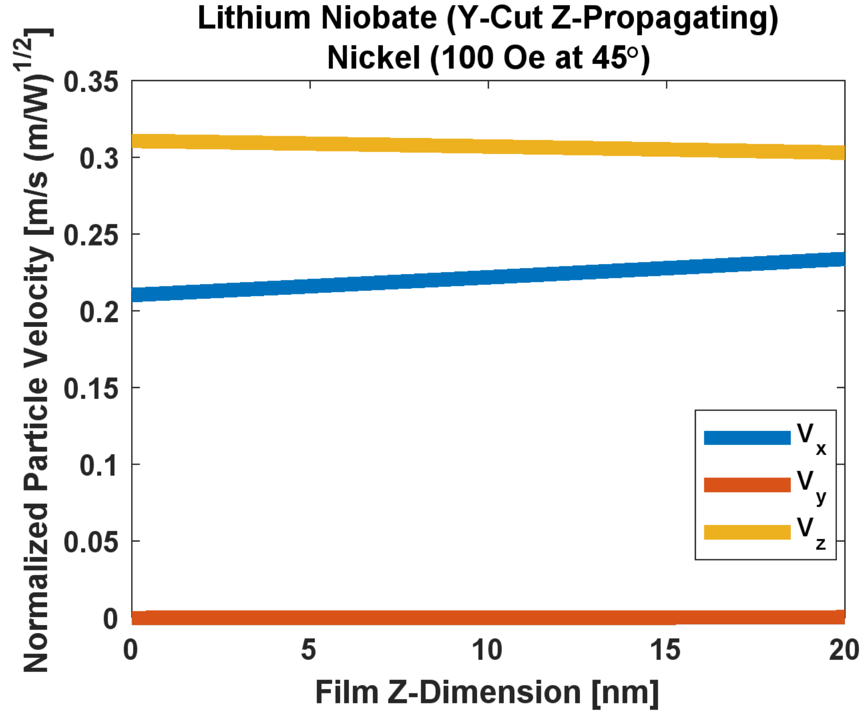

Results: Simple Delay Structures

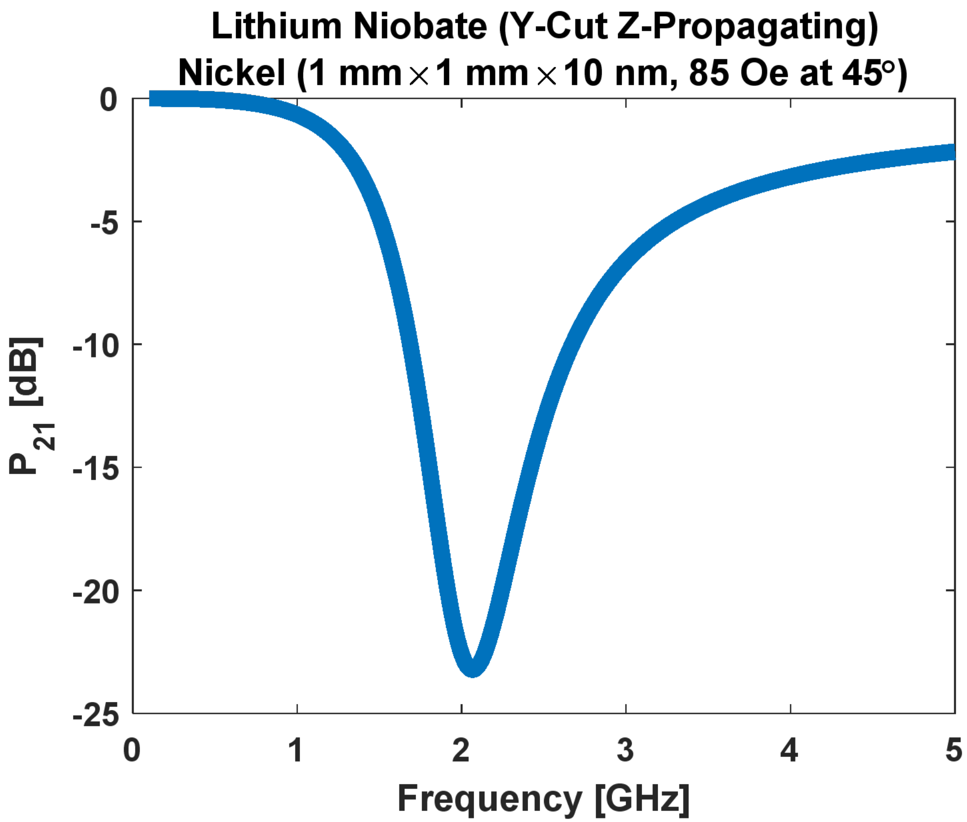

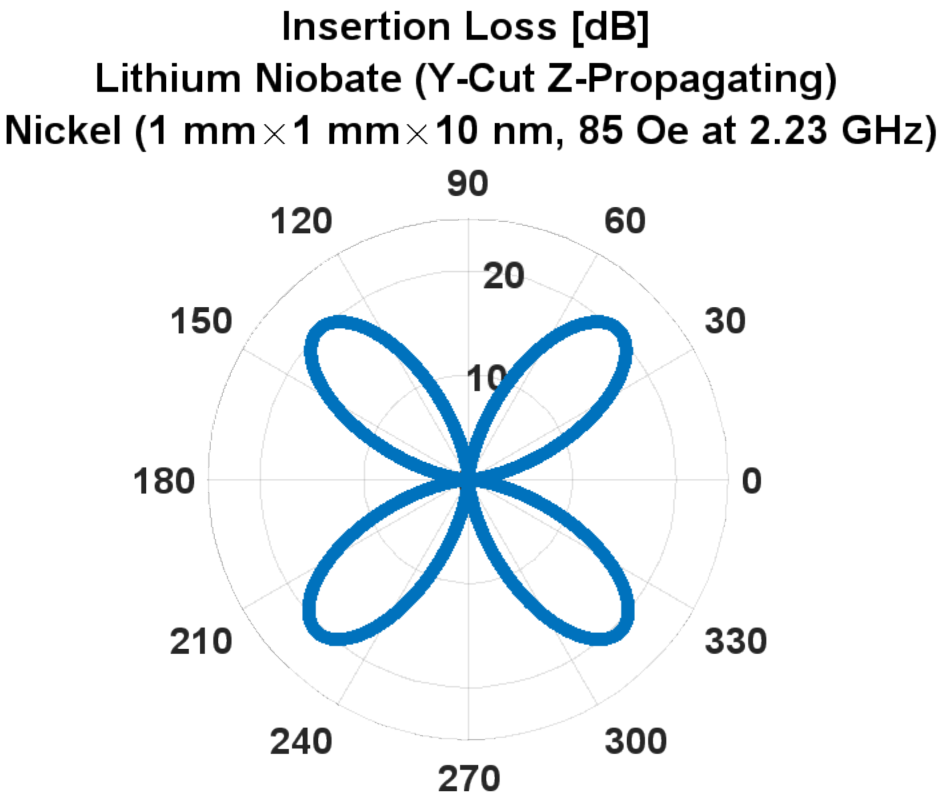

- ***1000 points (frequency or angle) are simulated between 0.25 - 1 seconds!***
- Model in it’s current state reproduce typical trends from ADFMR experiments but over predicts absorbed power (using literature material values)
- Improvements to the model (edge discontinuities, conductivity, nonuniform magnetization, etc) to improve quantitative accuracy are currently underway

Results: Mixed Delay + Bragg Structures

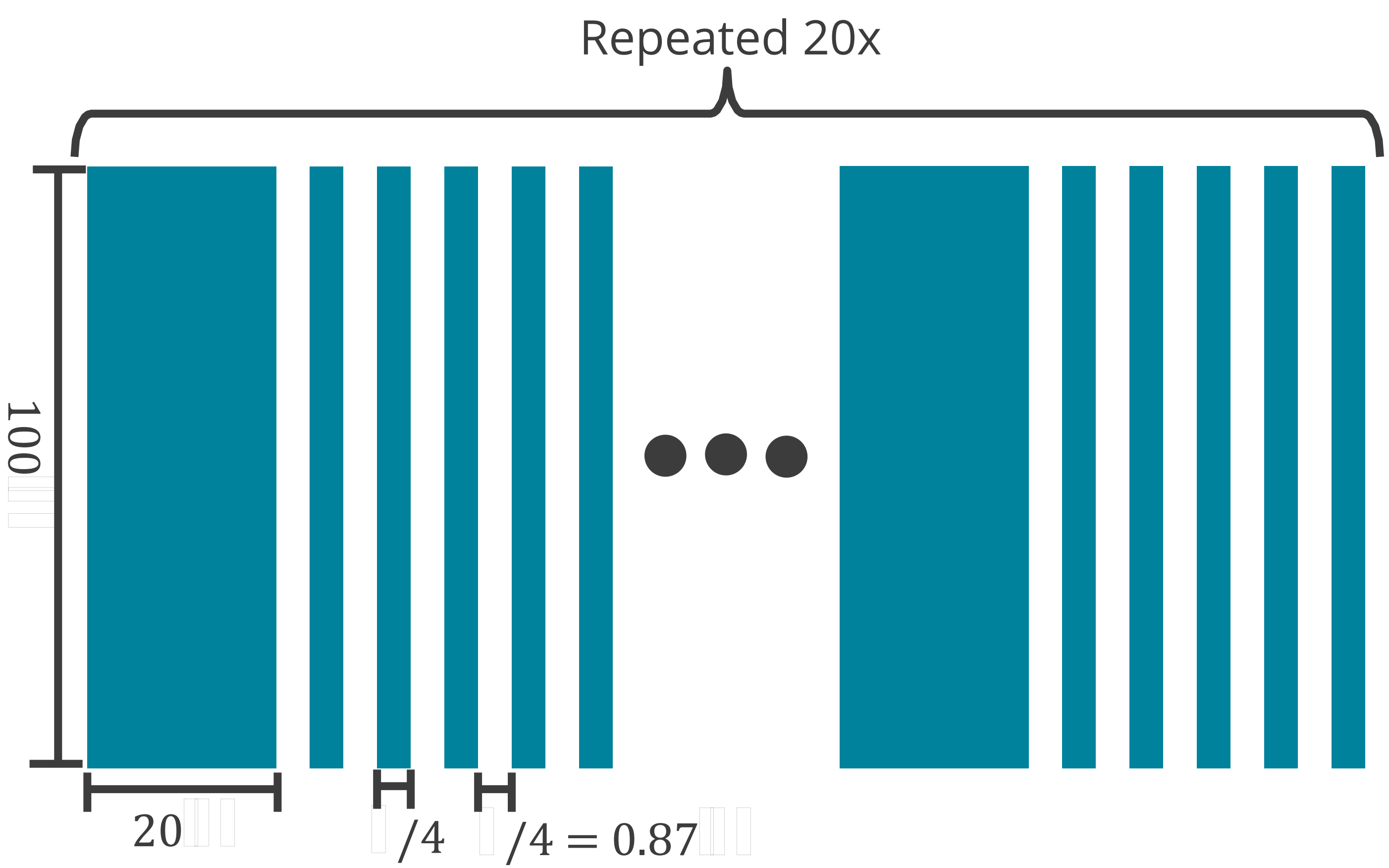

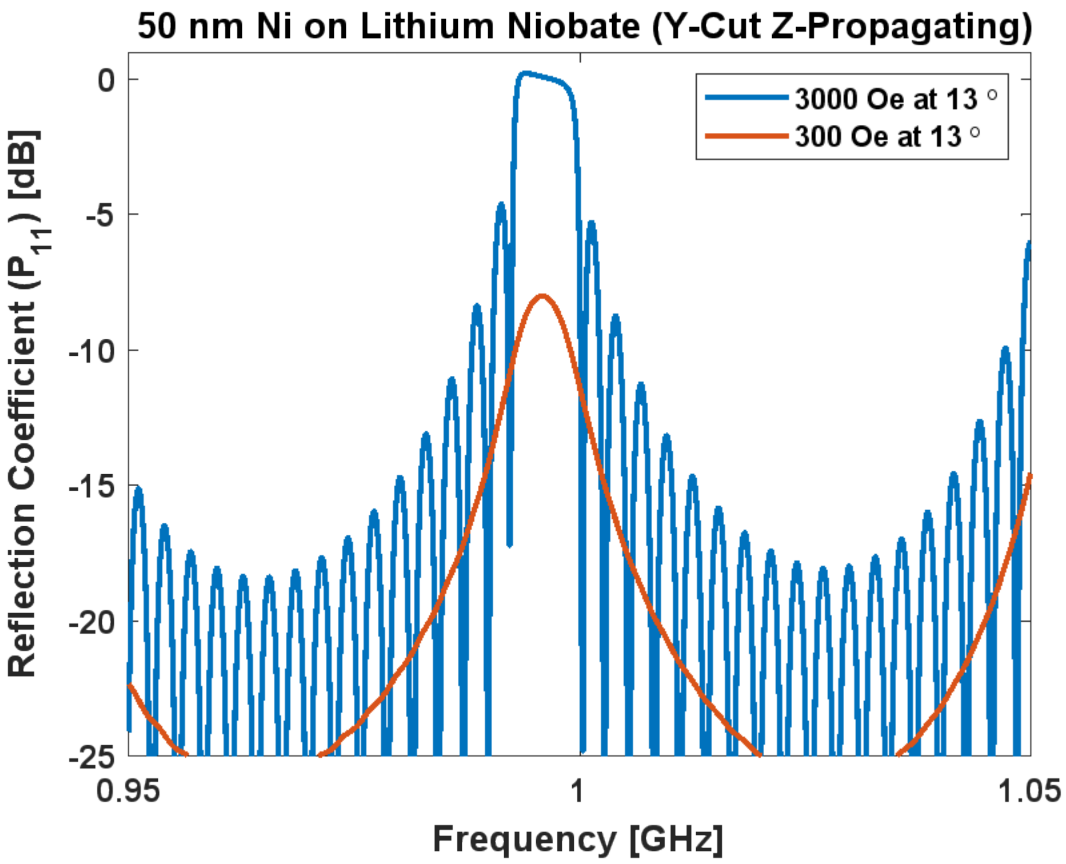

- For high bias fields, ferromagnetic resonance is far from the operating frequency and the structure behaves as a normal Bragg grating
- When bias is set to 300 Oe, ferromagnetic resonance aligns with the stop band and the reflection coefficient drops by 7.5 dB

Summary

- Traditional RF magnetic devices rely on electromagnetic wave interactions with the magnetic material, making them bulky as a result
- Leveraging magneto-elastic materials offers a route towards the miniaturization of RF magnetic devices, as the acoustic wavelength is 5 orders-of-magnitude smaller
- Lamb waves offer several advantages over SAWs for high frequency magneto-acoustic devices, such as higher velocities and coupling coefficients
- It has been demonstrated that magneto-acoustic interactions with Lamb waves is more akin to spin wave coupling than ADFMR
- To enable practical design of magneto-acoustic device, modelling techniques traditional to acoustic device design (such as the P-matrix method) must be adapted
- A perturbation based model for magneto-acoustic devices is derived, and it's utility in simulation of magneto-acoustic structures is demonstrated

Special thanks to all my PI's and collaborators!

Darren Branch, Aleem Siddiqui, Amun Jarzembski, Sean Bishop, Phil Mantos, Chris Nordquist, Joseph Schneider, Sebastian Wintz, Sri SPK Arekapudi, Kilian Lenz, Andres Chavez, Jürgen Lindner, Olav Hellwig, Greg Carman, Rob Candler

This work is supported by the National Science Foundation through the Cooperative Agreement for Solicitation NSF 11-537 (TANMS) managed by Dr. Sandra Cruz-Pol under Award EEC-1160504, and by the Sandia National Laboratories Laboratory Directed Research and Development. Sandia National Laboratories is a multimission laboratory managed and operated by National Technology and Engineering Solutions of Sandia, LLC, a wholly owned subsidiary of Honeywell International, Inc., for the U.S. Department of Energy's National Nuclear Security Administration under contract DE-NA0003525. The views expressed in the article do not necessarily represent the views of the U.S. Department of Energy or the United States Government.

Thank you!

Questions?